# The Effect of Manganese Additions on the Reactive Evaporation of Chromium in Ni-Cr Alloys

**Gordon R. Holcomb and David E. Alman**
Albany Research Center, U. S. Department of Energy
1450 Queen Ave. SW, Albany, OR 97321

## Abstract

Chromium is used as an alloy addition in stainless steels and nickel-chromium alloys to form protective chromium oxide scales. Chromium oxide undergoes reactive evaporation in high temperature exposures in the presence of oxygen and/or water vapor. The deposition of gaseous chromium species onto solid oxide fuel cell electrodes can reduce the efficiency of the fuel cell. Manganese additions to the alloy can reduce the activity of chromium in the oxide, either from solid solution replacement of chromium with manganese (at low levels of manganese) or from the formation of manganese-chromium spinels (at high levels of manganese). This reduction in chromium activity leads to a predicted reduction in chromium evaporation by as much as a factor of 35 at 800°C and 55 at 700°C. The results of evaporation loss measurements on nickel-chromium-manganese alloys are compared with the predicted reduction. Quantifying the effects of manganese additions on chromium evaporation should aid alloy development of metallic interconnects and balance-of-plant alloys.

## Introduction

The deposition of chromium onto solid oxide fuel cell (SOFC) electrodes is widely viewed as a major source of efficiency loss in fuel cells (1-3). Chromium bearing alloys, used as metallic interconnects or upstream in the balance of plant (BOP), form protective scales that contain chrome oxides. When chromium in the chrome oxides undergoes reactive evaporation in the presence of $O_2$ or $H_2O$, then chromium exists in the gas phase and is available for deposition on the SOFC electrodes. An example of a reactive evaporation reaction is Eq. 1.

$$½Cr_2O_3(s) + ¾O_2(g) = CrO_3(g) \quad (1)$$

Equation 1 is the formation of $CrO_3(g)$, which is the most prevalent chrome oxide gas specie when water vapor is not present. The vapor pressure of $CrO_3(g)$ is related to the activity of chromia ($Cr_2O_3$). Alloying elements in the alloy can lower the activity of $Cr_2O_3$, for example by substitution of Ni or Mn for Cr, or by the formation of $MnCr_2O_4$ spinel. The spinel is essentially a matrix of $Cr_2O_3$ and MnO.

In the case of alloying with Mn, the reduction of chromia activity, and thus the reduction of chrome evaporation, would be a maximum when sufficient Mn is available such that a continuous layer of spinel forms on the surface of the protective oxide. Smaller amounts of Mn would result in smaller reductions in chromia activity—but would still be of benefit. Too much Mn can be detrimental from an oxidation and physical property standpoint, thus the goal here is to quantify the benefits of Mn additions, so that alloy design for metallic interconnects or upstream BOP can optimize Mn content in the alloy.

The effectiveness of reducing the amount of chromium deposition onto SOFC electrodes is examined first from a theoretical basis by comparing the evaporation and thermodynamics of reactive evaporation from $Cr_2O_3$ with that from $MnCr_2O_4$. Secondly, long-term oxidation experiments were conducted on a series of Ni-25Cr-0.01Y-xMn alloys to indirectly measure the evaporation rate. Lastly, improvements in measuring the evaporation rate, using transport methods, are introduced.

## Evaporation

The reactive evaporation of $Cr_2O_3$ (or $MnCr_2O_4$) can be modeled in a variety of ways. The maximum evaporation rate can be found from Knudsen effusion (4), Eq. 2.

$$Evaporation\left(\frac{g}{cm^2\ \sec}\right) = \frac{m}{tA} = p\sqrt{\frac{M}{2\pi\pi R}} = 44.33\ p\ \sqrt{\frac{M}{T}} \quad (2)$$

Where m is the mass of the vapor generated (g), t is time (sec), A is surface area ($cm^2$), p is vapor pressure (atm), M is the molecular weight of the vapor (g/mol), T is temperature (K), and R is the gas constant. Thus, the evaporation rate is proportional to the vapor pressure of the gas specie.

Real evaporation rates can be many orders of magnitude lower than maximum evaporation rates. One way to determine real evaporation rates is to assume that volatility is limited by the transport of the volatile specie through a laminar boundary layer in the gas phase. For a flat plate geometry, the evaporation rate can be calculated by Eq. 3 (5-6):

$$Evaporation\left(\frac{g}{cm^2 hr}\right) = 0.664\,\mathrm{Re}^{0.5}\,\mathrm{Sc}^{0.33}\mathrm{D}\rho\,\mathrm{L}^{-1} \qquad (3)$$

Where Re and Sc are the dimensionless Reynolds and Schmidt numbers, D and ρ are the interdiffusion coefficient and density of the volatile specie in the boundary layer, and L is the characteristic length of the flat plate. When simplified (5), Eq. 3 becomes

$$Evaporation\left(\frac{g}{cm^2 hr}\right) \propto \frac{v^{0.5}}{P_T^{0.5}}p \qquad (4)$$

for low to moderate flow conditions and

$$Evaporation\left(\frac{g}{cm^2 hr}\right) \propto \frac{v^{0.8}}{P_T^{0.2}}p \qquad (5)$$

for turbulent high flow conditions ($Re > 3 \times 10^5$). In Eqs. 4-5, v is the linear gas velocity, $P_T$ is the total pressure, and p is the partial pressure of the evaporative gas specie. As with the maximum evaporation rate of Eq. 2, Eqs. 4-5 also show the evaporation rate proportional to p. So the thrust of the thermodynamic treatment is to determine the partial pressures of the evaporating gas species.

## Thermodynamics

There are a multitude of possible chromium-containing gas species that can be formed from $O_2$ and $H_2O$. These include Cr, $Cr_2$, CrH, CrO, $CrO_2$, $CrO_3$, $Cr_2O$, $Cr_2O_2$, $Cr_2O_3$, CrOH, $Cr(OH)_2$, $Cr(OH)_3$, $Cr(OH)_4$, CrO(OH), $CrO(OH)_2$, $CrO(OH)_3$, $CrO(OH)_4$, $CrO_2(OH)$, and $CrO_2(OH)_2$. The most important of these, in terms of highest partial pressures, are $CrO_3$, $CrO_2(OH)_2$, and $CrO_2(OH)$.

The Gibbs energy of formation, $\Delta G_f$, of each gas specie is used to determine its partial pressure over either $Cr_2O_3$ or $MnCr_2O_4$. For example, for the formation of $CrO_3$ over $Cr_2O_3$, Eq. 1, the partial pressure of $CrO_3$, $P_{CrO3}$, can by found from Eq. 6:

$$\Delta G_1 = \Delta G_{f,CrO_3} - \tfrac{1}{2}\Delta G_{f,Cr_2O_3} = -RT\ln\frac{P_{CrO_3}}{a_{Cr_2O_3}^{1/2} P_{O_2}^{3/4}} \qquad (6)$$

For pure $Cr_2O_3$, the activity of chromia, $a_{Cr2O3}$, is equal to 1. Another example is the formation of $CrO_2(OH)_2$ over $MnCr_2O_4$, Eqs. 7-9:

$$\tfrac{1}{2}MnCr_2O_4 + \tfrac{3}{4}O_2 + H_2O = CrO_2(OH)_2 + \tfrac{1}{2}MnO \qquad (7)$$

$$\Delta G_7 = \Delta G_{f,CrO_2(OH)_2} + \tfrac{1}{2}\Delta G_{f,MnO} - \tfrac{1}{2}\Delta G_{f,MnCr_2O_4} - \Delta G_{f,H_2O} \qquad (8)$$

$$\Delta G_7 = -RT\ln\frac{P_{CrO_2(OH)_2} a_{MnO}^{1/2}}{a_{MnCr_2O_4}^{1/2} P_{O_2}^{3/4} P_{H_2O}} \qquad (9)$$

Using equations similar to Eqs. 1 and 6, the partial pressures of $CrO_3$, $CrO_2(OH)_2$, and $CrO_2(OH)$ over pure $Cr_2O_3$ (activity of 1) were found for conditions of $P_{O2} = 0.2037$ and $P_{H2O} = 0.03$ (air plus 3% $H_2O$) and are shown in Fig. 1.

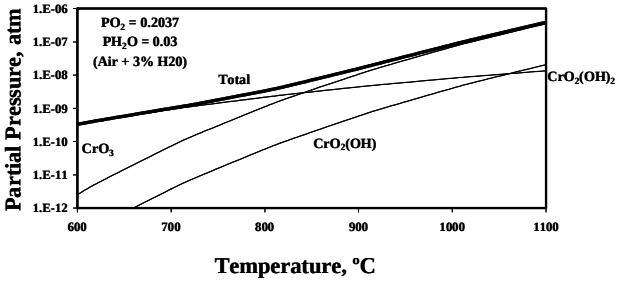


Fig. 1. The partial pressures of $CrO_3$, $CrO_2(OH)_2$, and $CrO_2(OH)$ over pure $Cr_2O_3$ air plus 3% $H_2O$.

Also shown in Fig 1 is the total partial pressure of gaseous chromium containing species. Except where noted, the thermodynamic data for these, and following, calculations are from the HSC Chemistry 5.11 database (7).

For similar calculations over $MnCr_2O_4$, the difficultly lies in the lack of $\Delta G_f$ data for $MnCr_2O_4$. Four values of $\Delta G_f$ (from $Cr_2O_3$ and MnO) were found in the literature at higher temperatures, Eqs. 10-13:

$$\Delta G_{f,\,MnCr2O4} = -59.376 \text{ kJ/mol at } 1100°C \text{ (8)} \qquad (10)$$

$$\Delta G_{f,\,MnCr2O4} = -59.0 \text{ kJ/mol at } 1250°C \text{ (9)} \qquad (11)$$

$$\Delta G_{f,\,MnCr2O4} = -42.278 \text{ kJ/mol at } 1300°C \text{ (10)} \qquad (12)$$

$$\Delta G_{f,\,MnCr2O4} = -52.600 \text{ kJ/mol at } 1600°C \text{ (11)} \qquad (13)$$

Taken together, the values of Eqs. 10-13 do not form a consistent relationship with respect to temperature. The values in Eqs. 10 and 13 were determined by similar methods of spinel-oxide phase equilibria: $MnCr_2O_4$-$CoCr_2O_4$ (8) and $MnCr_2O_4$-$MnAl_2O_4$ (11). Consequently, lower temperature values of $\Delta G_f$ were estimated using Eqs. 10 and 13. To make these estimates, the Newmann and Kopp rule (4) was used where the change in heat capacity, $\Delta C_p$, is equal to zero for condensed reactions. This allows the data in Eqs. 10 and 12 to be fitted to $\Delta G_T = \Delta H_{298} - T\Delta S_{298}$, where $\Delta H_{298} = -77.985$ kJ/mol and $\Delta S_{298} = -0.0136$ kJ/mol/K.

The total partial pressure of gaseous chromium containing species over pure $MnCr_2O_4$ was calculated and shown in comparison with the results over $Cr_2O_3$, Fig. 2 (in terms of maximum evaporation rate instead of total partial pressure). The data points in Fig. 2 represent the use of $\Delta G_f$ data of Eqs. 10-13 (8-11). The dotted line in Fig. 2 represents the use of estimated $\Delta G_f$ data as a function of temperature. Figure 2 shows the large reduction in Cr evaporation from a scale consisting of $Cr_2O_3$ to one having an outer layer of $MnCr_2O_4$. Without a continuous layer of $MnCr_2O_4$, or when the activity of $Cr_2O_3$ is less than one

because of Mn additions, the reduction in Cr evaporation would lie between the solid and dotted lines in Fig. 2.

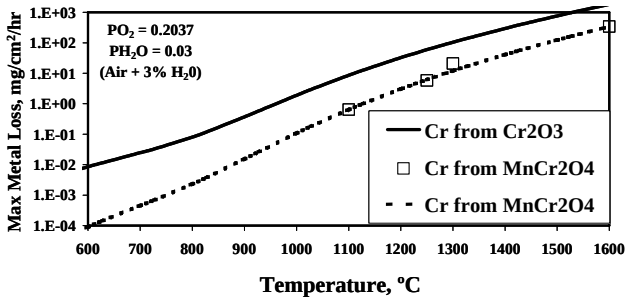


Fig. 2. The maximum evaporation rate of Cr over pure $Cr_2O_3$ and pure $MnCr_2O_4$ in air plus 3% $H_2O$. The data points represent the use of $\Delta G_f$ data of Eqs. 10-13 (8-11). The dotted line represents the use of estimated $\Delta G_f$ data as a function of temperature.

The calculations in Fig. 2 are for an environment of air plus 3% $H_2O$. When the calculations are repeated for other combinations of $P_{O2}$ and $P_{H2O}$, the total partial pressure and maximum evaporation rates change significantly, Table 1. Table 1 also shows similar calculations for the $NiCr_2O_4$ spinel. The conditions with the largest evaporation rates are when $O_2$ and $H_2O$ are both present.

Regardless of the values of $P_{O2}$ and $P_{H2O}$, the ratio of the maximum evaporation rate over a spinel to that over chromia (the reduction factors in Table 1) are only functions of temperature. The reduction factors for $MnCr_2O_4$ range from 18 at 1000°C to 95 at 600°C. The reduction factors for $NiCr_2O_4$ are all about 2.

## Experimental Procedures

A series of oxidation experiments were designed to measure the evaporation rates over Ni-25Cr alloys with various amounts of Mn additions. With these evaporation rates, experimental reduction factors could be compared with those calculated from thermodynamics.

The basis of the experiments was to conduct long-term oxidation tests at 950°C in air plus 5% water vapor until a steady-state scale thickness was reached and so subsequent mass loss measurements would measure the evaporation rate. Nickel-chromium alloys that form protective scales grow with parabolic kinetics, in which scale growth is inversely proportional to scale thickness. Combining this with constant evaporation rates that are independent of scale thickness, there should come a time where scale growth from oxidation matches scale loss from evaporation—thus producing a steady-state scale thickness. An elevated temperature of 950°C was used to increase the evaporation to a more readily measurable rate.

Five Ni-25Cr alloys were produced melted and rolled to have nominal compositions of Ni-25Cr and Ni-25Cr-0.01Y-xMn, with x equal to 0, 0.4, 1, and 3. It was thought that scale adhesion could be improved by the addition of a small amount of Y. The actual compositions are shown in Table 2.

Table 1. The maximum evaporation rates of Cr from $Cr_2O_3$, $NiCr_2O_4$, and $MnCr_2O_4$ for a varitey of temperatures, $P_{O2}$, and $P_{H2O}$ values. Also shown are the reduction factors (ratios) for $NiCr_2O_4$, and $MnCr_2O_4$ compared with $Cr_2O_3$

| Temperature, °C | Maximum Cr Loss, mg/cm²/hr, from $Cr_2O_3$ | $NiCr_2O_4$ | $MnCr_2O_4$ | Reduction Factor from $NiCr_2O_4$ | Reduction Factor from $MnCr_2O_4$ |
|---|---|---|---|---|---|
| $P_{O2} = 0.21$, $P_{H2O} = 0$ | | | | | |
| 600 | 0.0000728 | 0.0000390 | 0.000000766 | 1.9 | 95 |
| 700 | 0.00199 | 0.00105 | 0.0000365 | 1.9 | 55 |
| 800 | 0.0290 | 0.0150 | 0.000832 | 1.9 | 35 |
| 900 | 0.264 | 0.135 | 0.0110 | 2.0 | 24 |
| 1000 | 1.67 | 0.845 | 0.0953 | 2.0 | 18 |
| $P_{O2} = 0.20$, $P_{H2O} = 0.05$ | | | | | |
| 600 | 0.0140 | 0.00751 | 0.000148 | 1.9 | 95 |
| 700 | 0.0393 | 0.0206 | 0.000718 | 1.9 | 55 |
| 800 | 0.113 | 0.0583 | 0.00323 | 1.9 | 35 |
| 900 | 0.433 | 0.221 | 0.0180 | 2.0 | 24 |
| 1000 | 2.01 | 1.02 | 0.115 | 2.0 | 18 |
| $P_{O2} = 0.10$, $P_{H2O} = 0.20$ | | | | | |
| 600 | 0.0332 | 0.0178 | 0.000350 | 1.9 | 95 |
| 700 | 0.0898 | 0.0472 | 0.00164 | 1.9 | 55 |
| 800 | 0.216 | 0.112 | 0.00620 | 1.9 | 35 |
| 900 | 0.560 | 0.286 | 0.0233 | 2.0 | 24 |
| 1000 | 1.80 | 0.908 | 0.102 | 2.0 | 18 |
| $P_{O2} = 0.001$, $P_{H2O} = 0.344$ | | | | | |
| 600 | 0.00181 | 0.000967 | 0.0000190 | 1.9 | 95 |
| 700 | 0.00487 | 0.00256 | 0.0000892 | 1.9 | 55 |
| 800 | 0.0116 | 0.00601 | 0.000333 | 1.9 | 35 |
| 900 | 0.0291 | 0.0149 | 0.00121 | 2.0 | 24 |
| 1000 | 0.0900 | 0.0454 | 0.00513 | 2.0 | 18 |

Table 2. Composition of experimental alloys, wt%.

| Alloy | Ni | Cr | Mn | Y |
|---|---|---|---|---|
| G1 | 74.4 | 24.9 | 0.026 | 0 |
| G2 | 74.7 | 24.6 | 0.020 | 0.050 |
| G3 | 74.1 | 24.8 | 0.46 | 0.063 |
| G4 | 71.5 | 26.4 | 1.44 | 0.083 |
| G5 | 71.6 | 24.3 | 3.49 | 0.130 |

The samples were cut into pieces with dimensions of approximately 1.5 cm x 0.9 cm x 0.3 cm, and the surfaces ground to 600 grit. The samples were placed inside alumina crucibles and heated to 950°C in an alumina tube furnace. Water was added to a preheating chamber with a metering pump and fed into the furnace along with air. The gas mixture was nominally 5% water vapor and flowing at approximately 10 cm/min. Periodically the furnace was cooled and the samples removed for weighing, then put back into the furnace to heat back up to temperature. The furnace was heated and allowed to cool at a rate of 200°C/hr.

## Experimental Results

The results of the mass change measurements are shown in Fig. 3. However, the negative slopes for several of the alloys after 500 hours do not represent the evaporation rate. The samples were observed to be spalling, with a fine power collecting inside the crucibles.

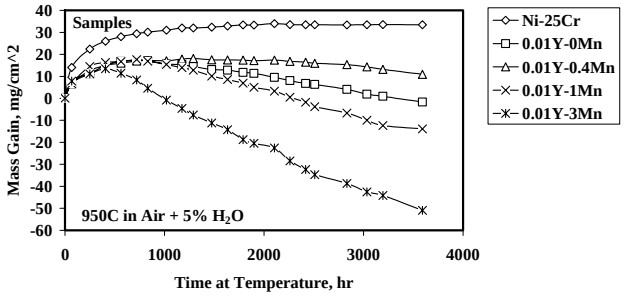


Fig. 3. Mass change with time for the five Ni-25Cr-Y-Mn alloys oxidized in air + 5% $H_2O$ at 950°C.

Subsequent to the observation of spalling, the total mass of each sample and crucible was collected, Fig. 4. The slopes of the lines continue to either increase or to remain flat. The conclusion was that the spalling was continuing and allowing oxidation to occur at a faster rate than evaporation. Thus the evaporation rate could not be obtained from these results.

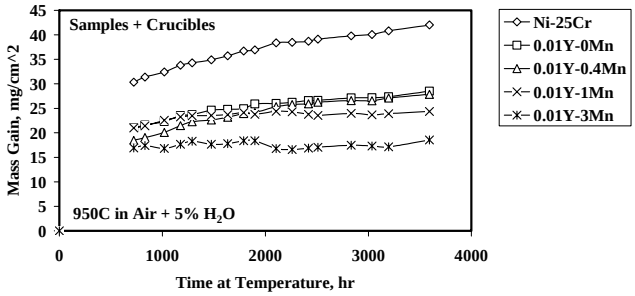


Fig. 4. Mass change with time for the five crucibles plus the Ni-25Cr-Y-Mn alloys oxidized in air + 5% $H_2O$ at 950°C.

## Future Work

A more direct measurement of the evaporation rate is planned using the transpiration method (4,12). In this method, chromium gas species are generated from the oxide in a flowing gas stream. The chromium gas species travel through a capillary and collected by condensation outside the furnace. One example of the successful use of this method is by Gindorf et al. (12), who measured Cr evaporation from the oxide dispersive (ODS) alloy Cr-5Fe- $1Y_2O_3$. They obtained a rate of 8.6 µg/h with an 80 mm x 30 mm x 5 mm sample for flow rates above 1.5 l/min in air at 950°C. This is equivalent to $4.05 \times 10^{-11}$ g/cm$^2$/s.

## Summary

The goal was to quantify the benefit from additions of Mn in alloys for SOFC components to reduce the evaporation rate of Cr. Thermodynamic calculations resulted in a maximum benefit of reducing the evaporation rate by a factor of 18 at 1000°C to as much as a factor of 95 at 600°C. The maximum benefit was calculated assuming sufficient Mn to form a continuous layer of $MnCr_2O_4$ on the surface of the scale. Additions of less Mn would result in a lower reduction factor.

Similar calculations were done assuming a spinel of $NiCr_2O_4$. The reduction factor here was about 2—much less than for $MnCr_2O_4$.

An experimental verification of these reduction factors was attempted using long-term oxidation studies to indirectly measure the evaporation rate. Spalling of the oxide scales prevented the establishment of parabolic kinetics, so a balance in scale growth from oxidation with scale loss from evaporation was not established. Consequently, the evaporation rates were not measured.

Future work is planned to measure the reduction factors using the transpiration method

## References


1. K. Hilpert, D. Das, M. Miller, D. H. Peck and R. Weiß, *J. Electrochem. Soc.,* 143, 3642-3647 (1996)
2. S. P Jiang, J. P. Zhang and K. Föger, *J. Electrochem. Soc*., 147, 3195 (2000).
3. S. P. Jiang, J. P. Zhang, L. Apateanu and K. Föger, *J. Electrochem. Soc*., 147, 4013 (2000).
4. O. Kubaschewski and C. B. Alcock, *Metallurgical Thermochemistry*, pp 127-131, 139-143, 184, Pergamon Press, Elmsford, New York (1979)
5. E. J. Opila, *Materials Science Forum*, Vols. 461-464, 765-774 (2004)
6. G. H. Geiger and D. R. Poirier, *Transport Phenomena in Metallurgy*, pp. 529-532, Addison-Wesley, Reading, Massachusetts (1973)
7. A. Roine, *HSC Chemistry 5.11*, Outokumpu Research Oy, Pori, Finland (2002)
8. K. T. Jacob and K. Fitzner, *J. Mat. Sci*., 12, 481-488 (1977)
9. J. V. Biggers, "Experimental Determination of Some Thermodynamic Properties of Oxide Solid Solutions Containing MnO and CoO," Ph.D. Thesis, Pennsylvania State University, University Park, Pennsylvania (1966)
10. N. Koc, Activity-Composition Relations in $MnCr_2O_4$-$CoCr_2O_4$ Solid Solutions and Stabilities of $MnCr_2O_4$ and $CoCr_2O_4$, Ph.D. Thesis, Middle Ease Technical University, Ankara, Turkey (1993)
11. H.-T. T. Tsai and A. Muan, *J. Am. Cer. Soc*., 75, 1407-1411 (1992)
12. C. Gindorf, L. Singheiser, K. Hilpert, M. Schroeder, M. Martin, H. Greiner and F. Richter, *Solid Oxide Fuel Cells (SOFC VI),* Proceedings of the Sixth International Symposium, Proceedings Volume 99-19, 774-782, Eds. S. C. Singhal and M. Dokiya, Electrochemical Society, Pennington, New Jersey (1999)